Immersion white light scanning interferometry using elastic polymer path length compensation

Mukhtar Husneni, Paul Montgomery, Freddy Anstotz, Rémi Barillon, Anne Rubin

Immersion white light scanning interferometry using elastic polymer path length compensation

Husneni Mukhtar[a,b], Paul Montgomery[a], Freddy Anstotz[a], Rémi Barillon[c], Anne Rubin[d]
[a]ICube Laboratory, University of Strasbourg-CNRS, 23 rue du Loess, 67037 Strasbourg, France; [b]Telkom University, Jl.Telekomunikasi Terusan Buah Batu, 40257 Bandung, Indonesia; [c]Institut Pluridisciplinaire Hubert Curien (IPHC), University of Strasbourg-CNRS, 23 rue du Loess, 67037 Strasbourg, France; [d]Institut Charles Sadron, CNRS, 23 rue du Loess, 67037 Strasbourg, France

ABSTRACT

Improvements have been made to a commercial Linnik microscope in order to perform measurements in water for studying structures of transparent and non-transparent samples. One of the main goals of the present work is to study pollutants in colloidal layers immersed in liquid. The second reason to work in liquid is to increase the lateral resolution. The challenges to overcome include achieving stability in the complex Linnik design as well as the difficulty of balancing the optical distance of the two arms of the interferometer to obtain the interference fringes. The main problem is the path length compensation in the mirror arm which needs a complex mechanical design to allow a high enough number of degrees of freedom for to correct alignment of the optical elements. In our system, the reference mirror arm is mounted horizontally, making liquid immersion tricky. In this work, we have investigated alternative solutions based on non-liquid elastic polymers placed between the end of the objective and the reference mirror using sodium polyacrylate (SPA) beads and PDMS (polydimethylsiloxane) slabs, with a refractive index very close to that of water. The results of the performance tests of the modified system are presented and demonstrated. The new design provides a workable system that is ready for the future study of colloidal and other samples directly in water.
Keywords: WLSI, CSI, surface topography, immersion, Linnik design, path length compensation

1. INTRODUCTION

White Light Scanning Interferometry (WLSI) or Coherent Scanning Interferometry (CSI), a well-known non-contact optical profiler for measuring surface topography, is normally carried out in air. A Linnik design allows the use of higher power objectives, typically from ×50 to ×200 or lower, because no component is required between the objective and the sample. One requirement for this design is that the optical path lengths of the two arms need to be equal, thus necessitating separate adjustment of the optical path length difference and focusing of the reference mirror and sample, which are not easy[1]. Its sensitivity to mechanical influences is another reason why the Linnik arrangement is rarely used and rather limited in commercial use[2,3]. However, this design is selected for implementation due to several advantages[1,4,5] such as independent adjustment of optical path lengths and focusing in both arms, the use of a wider numerical aperture to improve lateral resolution, easier insertion of components on the sample as well as the reference mirror arms and the use of wave plates in the separate interferometer arms together with a polarizing beam splitter (PBS).

[6]. The use of the PBS allows the splitting of the light into reflected s-polarized and transmitted p-polarized beams, providing the advantage of simplifying the intensity balance betweenn the reference mirror and the different sample reflectivities[7,8]. While a Mirau design is inherently more stable due to the use of a single objective[9] and is free from dispersion errors due to the same thickness of the plane-parallel plates[8], it is limited to medium magnification objectives and use in air.

Although CSI has nanometric axial resolution for measuring surface height, the lateral resolution is limited by diffraction to about $\lambda/2$. When studying structures in transparent samples or samples in liquid, dispersion mismatch distorts the fringe envelope and makes measurements difficult or impossible due to the separation of the coherence gate from the focus gate.

In this work, we have modified a commercial Linnik microscope (Fogale-Nanotech OEM system)[10] in order to extend the measurement modes of the CSI technique to be able to cope with samples in a liquid medium so as to improve the lateral resolution and to be able to study pollutants in colloidal layers and other materials in liquid. The challenges to overcome

include achieving stability in the complex Linnik design and the difficulty of balancing the optical distance of the two arms of the interferometer to obtain the interference fringes superimposed on to a focused image of the submerged substrate.

The modification of the original microscope has involved finding a balance between having a high enough number of degrees of freedom(?2 degrees in the lateral, 2 degrees for the orientation and 1 degree in the path length) for the mechanical adjustments to correctly align the interferometer and being simple enough to be practically usable. Both the object arm and reference mirror arm designs have been studied and improved.

The new Linnik configuration uses two identical water-immersion microscope objectives in each of the reference and object arms with a broadband white light LED for the light source. With the objective and sample both immersed in water, it is also necessary to compensate the reference arm. One way of doing this is by using a glass plate[11-13], which enhances the visibility of the interferogram, but still introduces a slight dispersion mismatch. Another way is to use water between the objective lens and mirror. But as in most Linnik designs, the reference arm is mounted horizontally, making the use of water mechanically tricky. Instead, we have investigated alternative solutions based on non-liquid elastic polymers placed between the end of the objective and the reference mirror. The first one consists of adapted sodium polyacrylate (SPA) beads, with a refractive index very close to that of water and the second consists of polydimethylsiloxane (PDMS) slabs with a refractive index in the range of 1.335 to 1.400.

Another important modification is the use of a motorised stage in the reference arm for automatically finding the fringes and simplifying the alignment. The results of the performance tests of the modified system are presented and demonstrate improved lateral resolution compared with measurements made in air. The new design provides a workable system that is ready for the future study of colloidal and other samples directly in water.

2. EXPERIMENTAL

In this section, the experimental work is described including the sample used in the measurements, the techniques used for path length compensation and the configuration of the water immersion Linnik. The results of measuring samples in water are demonstrated, as well as the comparison with measurements from other microscopes.

2.1 Immersion Linnik system measurements

The primary measurement system constructed and modified for measuring in liquid is the new water immersion Linnik, shown schematically in Figure 1. A water-immersion objective and a reference mirror are placed in the reference beam arm while the other water-immersion objective and sample are placed in the object beam arm. The sample to be measured is placed in a container filled with distilled water. The measurement system is controlled by a PC with Intel® Xeon® CPU processor (2.40 GHz, 8 GB RAM) and Windows 7 operating system (64-bit). The control and analysis software "CPM 2015" was developed internally in LabVIEW (2014 version, 64-bit, National Instruments), combined with the IMAQ Vision module.

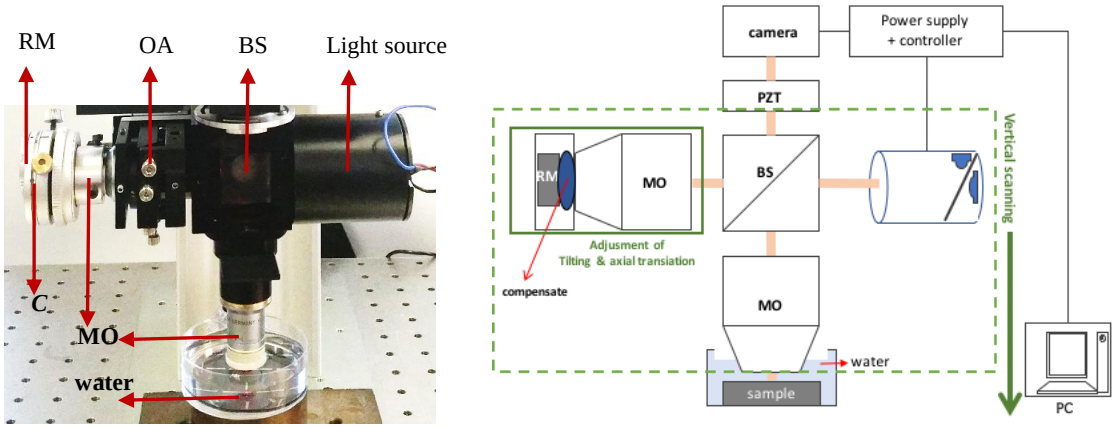

Figure *1*. Photograph of water immersion Linnik head (left) and the layout of the experimental arrangement of water-immersion Linnik configuration (right). BS, beam splitter (broadband, non-polarizing); MO, microscope objective (water immersion); OA, optical adjustment; C, compensator, RM, reference mirror (80% reflectivity); PZT, piezo translation.

The illumination source consists of a white light LED with ao center wavelength of 568 nm and spectral width of 100 nm at FWHM. The measured effective wavelength in water is 450 nm, due to the Köhler illumination. The beam is split by a non-polarizing cube beam splitter with R/T= 45/45 to the reference arm and to the object arm. The reflected beams from both arms are collected through the same beam splitter and recorded by the monochrome CMOS camera (Photonfocus MV1-D2048-96-G2 with 2048 × 2048 pixels) with a Giga Ethernet connection and a frame rate capability of 22 images per second. Objectives of ×20 and ×40 magnification are used, with working distances of 3.5 mm and 3.3 mm respectively. With the NA of 0.5 and 0.8 of the objectives, the Rayleigh criterion results in lateral resolutions of 0.41µm for the ×20 objectives and 0.25 µm for the ×40 objectives when measuring in water. The reference and sample objectives must be accurately focused on the reference mirror and on the sample respectively in order to obtain good fringes.

To perform the CSI measurement of the sample, the piezo is used to move the interferometer head so as to scan the interference fringes over the full depth of the sample roughness. The scanning step used is $\lambda_{eff}/8$, where λ_{eff} is the effective wavelength. This corresponds to the $\pi/2$ phase step necessary for use with the five step adapative (FSA) algorithm for fringe envelope determination. An interpolation method was used to improve the axial resolution. The results were analyzed using Mountains Map v6 from Digital Surf to produce false color images of the altitude data, 3D image and the line profile of the surface.

2.2 Other microscopes used for comparison

Comparisons were made with the measurements from three other profiling microscopes so as to test the new immersion Linnik system. The first was an AFM microscope using the non-contact mode, the second, a Zygo NewView 7200 with a x50 Mirau objective and the third, a modified Leitz-Linnik microscope with x50 objectives. The specifications[17] are presented in Table 1.

Table *1*. The microscope specification used for comparison results of measurement

Microscope	Resolution
AFM (Park XE70) non-contact mode	$r_{lateral}$ = 0.012 µm – 0.195 µm depending on the field size
Zygo NewView 7200, ×50 Mirau	$r_{lateral}$ = 0.52 µm
Leitz-Linnik microscope, ×50 Linnik	$r_{lateral}$ = 0.43 µm

2.3 Sample preparation

Two types of samples were used to test the new water immersion Linnik system. The first was an etched silicon wafer[8] made using a mask with UV photolithography and RIE etching. The second was a colloidal sample of aluminum or commonly called alumina. This is a chemical compound of aluminum oxide (Al_2O_3). This alumina compound is mixed in water and placed on the surface of a glass plate, then allowed to dry. Different alumina concentrates i.e. 1 g/l, 2.9 g/l, and 14 g/l, were produced to observe the distribution of alumina in suspension and the size of the alumina aggregates.

2.4 Path length compensation

As previously stated, water can be used in a reservoir to compensate the reference arm, for example by making a tank that can be fixed to the horizontal reference objective[14,15]. While this has good results for imaging in skin, it has the inconvenience of water leakage. The self-supporting material we propose using between the reference objective and mirror that have a refractive index close to that of water, are SPA and PDMS. The measured values of refractive index of SPA and PDMS measured manually by an Abbe-refractometer are 1.335 and 1.401 respectively.

SPA, known as "water lock" and "water beads", is a polymer that has the remarkable ability to absorb as much as 100 to 1000 times its mass in water. These beads, shown in Figure 2(a), are commonly used in some fields such as in health care (sanitary towels, paper diaper, medical bandage), industry or agronomy for retaining moisture in cultures in dry regions or in potted plants.

In our application, SPA can be used as a substitute for water in both arms or only in the reference arm, as shown in Figure 2(b) and Figure 2(c). As far as we know, this type of path length compensation for interference microscopy has not yet been reported in the literature. In practice, a 3-mm-diameter SPA bead is placed between the reference mirror and the

objective after being cut to the thickness of the working distance of the objective used (3.5 mm and 3.3 mm respectively for the ×20 and ×40 objectives).

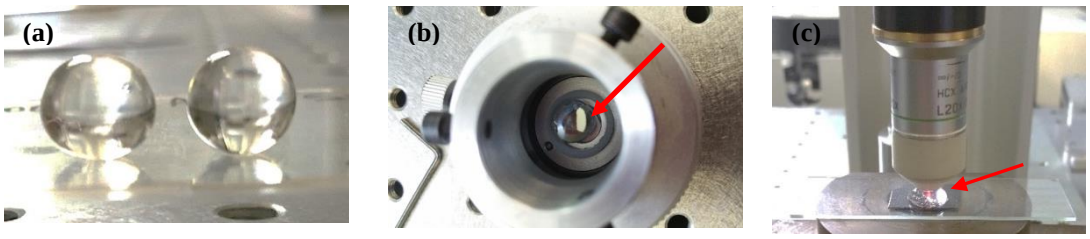

Figure 2. (a) SPA beads, (b) SPA contacts with reference mirror, (c)SPA is between sample and the object objective.

The advantages of using SPA are its ease of use and application in the reference arm, its ability to provide a refractive index close to that of water and the stability in its form at a maximum temperature of 25°C. The only inconvenience in using this material is the bead needing to be changed after a few hours or days because of water evaporation.

The second polymer material studied is PDMS, a Si based organic polymer made of a group of polymeric organosilicon compounds, also known as dimethicone, that is optically transparent, inert and non-toxic. The main advantages of using this material in our application are its viscoelasticity, enough flexibility to manipulate across macroscopic scales, bio-compability, high chemical inertness, optical transparency, adhesion to metals, applications as inert substrate material and being stable at room temperature.

Unlike SPA, PDMS requires several steps of preparation before it can be used as a compensator in the reference arm. It is necessary to design the PDMS slab with the correct size so that it is suitable for the variation in working distance of each objective magnification. We therefore made a specific mold out of Teflon for forming the PDMS as shown in Figure 3. A glass plate formed the base of the mold during molding of the PDMS compound.

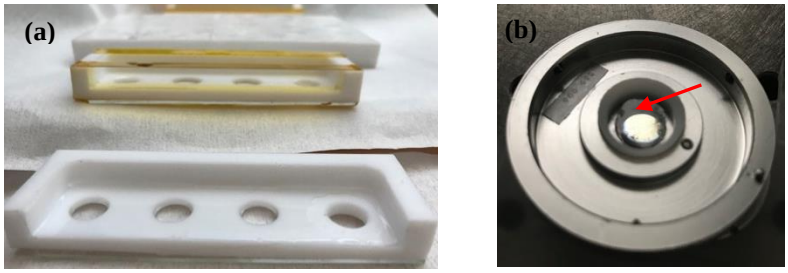

Figure 3. (a) Molds of PDMS slabs in variation of height to suit the working distance of objective lens, (b) PDMS contacts with reference mirror.

Bluesil RTV 141 was used to make the PDMS by mixing the two components. Both the PDMS base and catalyst or curing agent are scaled with a certain mass ratio. A degassing process was employed to remove bubbles after well mixing the components, before pouring the mixture into the mold, curing with an oven and drying at room temperature.

One of the requirements that needs to be considered in the preparation of the PDMS slab as a medium is that it should present an optically flat, smooth and transparent surface without marks or scratches. Furthermore, the PDMS slab should have a sufficient elasticity in order to avoid the possibility of excessive pressure on the optical components when performing the measurements. The sufficient elasticity is necessary to safely apply the PDMS on to the reference mirror. After performing experimental tests with different concentrations, we obtained a ratio with a satisfactory elasticity of PDMS of 25 : 1 for the PDMS base to catalyst, compared with the commonly used ratio of 10 : 1.

As for the SPA, PDMS can then be used as a compensator. Having a non-liquid form, both of them can easily be placed in a vertical position between the reference objective and the reference mirror. However, for long term utilization, the

PDMS should be stored at a temperature of less than 20° C so as not to become too hard (the result of experimental observation), making it unsuitable for use in the reference arm.

3. RESULTS AND DISCUSSION

Firstly, the measurement results using the two compensation solutions proposed are presented. Then, a comparison is made between the results of the measurements of the immersion Linnik system with those from other microscopes.

3.1 Measurement using elastic polymers

The advantages and disadvantages of the experimental preparation using SPA and PDMS have been described in the previous sections. In this section, we present the measurement results using these elastic polymers for measuring the samples in water. The polymer is placed between the reference mirror and the reference objective. Figure 4 shows the reference objective focused on the reference mirror using each polymer with the ×20 objective, scratches and marks on the reference mirror being visible that help in focusing the reference objective. It can be seen that the SPA gives a sharper image of the reference mirror than that using the PDMS. This may be due to an inaccuracy in the PDMS thickness or to the polymer being slightly translucent and diffusing the light. In the case of using the SPA, it is not necessary to cut it with such a high accuracy of thickness. On the other hand, SPA will break due to the pressure between the objective and reference mirror if it is too thick. However, these two polymers are able to provide the surface profiling results as shown in and Figure 6.

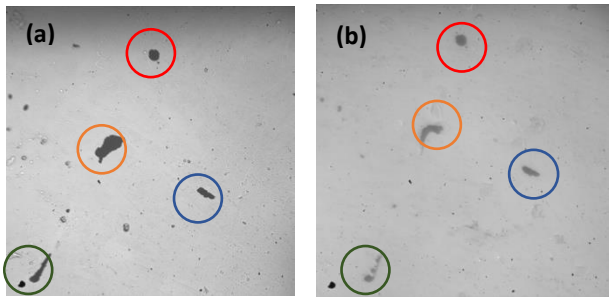

Figure 4. Focus of the reference objective on reference mirror. An elastic polymer of (a) SPA and of (b) PDMS is placed between the reference mirror and the objective.

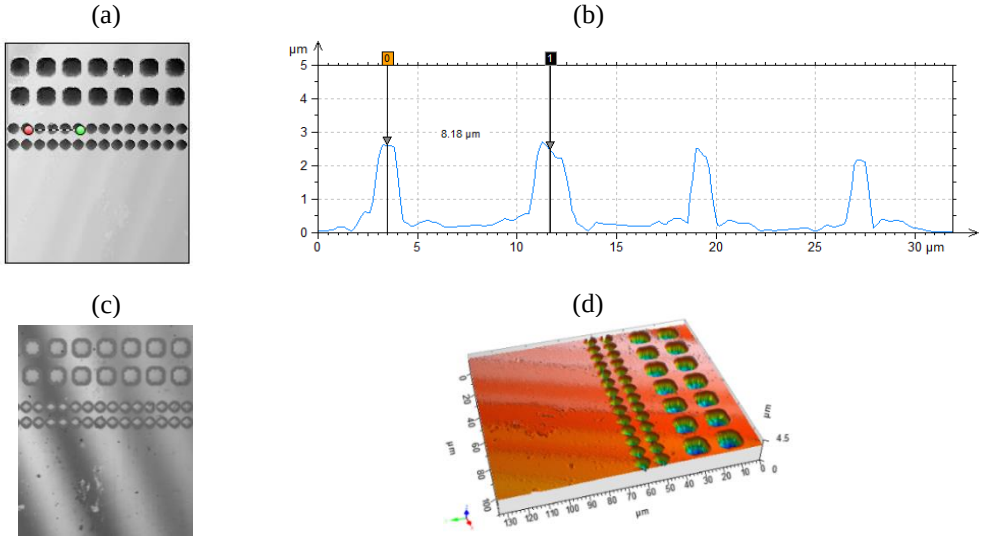

Figure 5. Etched Silicon, 8 µm and 2.5 um of depth and width of valley respectively, is measured with ×40 water immersion Linnik system (NA=0.8, λ_{eff}=450 nm) with SPA placed in the reference arm. (a),(b) line profile on measured area; (c) fringe image; (d) 3D image.

The results of these experiments is that the use of SPA in the reference arm provides a convenient solution to path length compensation. Compared to PDMS, SPA is able to provide better fringe contrast and better profiling results. In addition to being easy to obtain, this material not only offers the time efficiency in finding the focus of the reference objective but is also to present a better compensation of path length for producing good results. However, the use of PDMS leads to a degradation in the quality of the results (Figure 6), which requires further studies to see if it could provide a satisfactory solution.

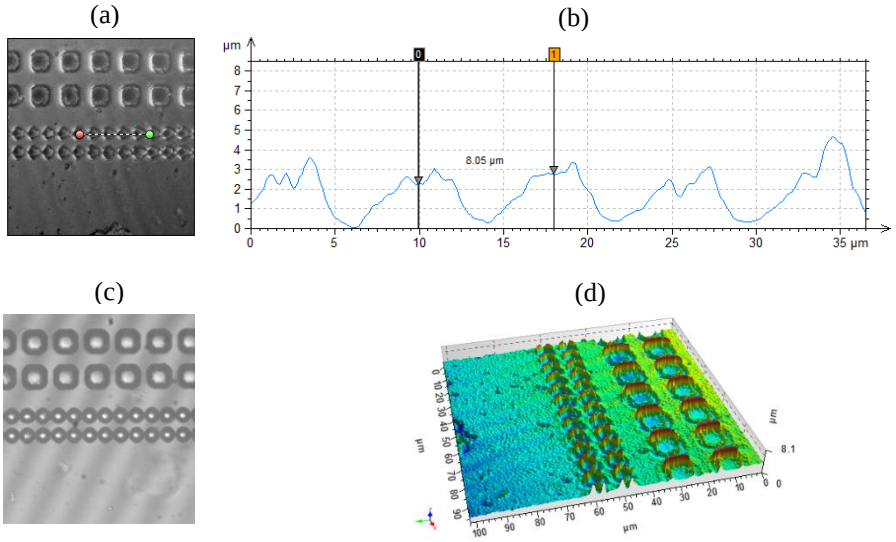

Figure 6. Etched Silicon, 8 µm and 2.5 um of depth and width of valley respectively, is measured with ×40 water immersion Linnik system (NA=0.8, λ_{eff}=450 nm) with3.25 mm thickness of PDMS placed in the reference arm. (a), (b) line profile on measured area; (c) fringe image; (d) 3D image.

3.2 Comparison measurements with other microscopes

A standard calibration of RS-N SiMETRICS was used to measure the lateral resolution experimentally. Values of 1.2 µm and 0.8 µm lateral resolution were obtained for the ×20 and ×40 immersion objectives respectively, while the theoretical lateral Rayleigh resolutions are 0.41 µm and 0.25 µm.

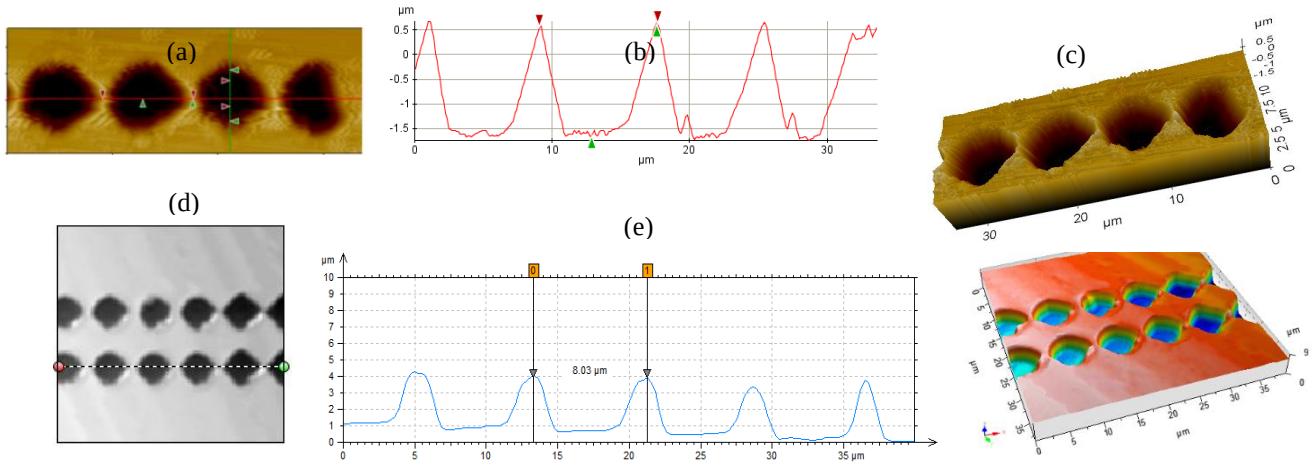

Figure 7. Etched Silicon, 6 µm and 2.5 um of width and depth of valley respectively, is measured using (a), (b), (c) in air using AFM microscope (Park XE 70 model, non-contact mode) and (d), (e), (f) ×20 water immersion Linnik system (NA=0.5, λ_{eff}=450 nm).

Results of the measurements of the samples made with the different microscopes are shown in *Figure 7* to *Figure 9*. These results show a better lateral resolution and better image quality for the measurements made in water.

The results of the measurements of the hole patterns etched in Silicon using AFM and the ×20 immersion Linnik are shown in *Figure 7* for comparison. The width and depth of the valley are around 8 µm and 1.5 µm for both microscopes in the same area of the sample surface. In *Figure 8*, the measurements of a grating etched in silicon with a 10 µm pitch using the ×50 Mirau Zygo microscope and ×40 immersion Linnik are shown. Both images show similar results, with a 10 µm pitch and 2.2 µm depth. Nonetheless, there are errors in the profiles in *Figure 8* (c) on the top and bottom surfaces because of the batwing effect. This might be caused by shadowing and the way the illumination light diffracts at the discontinuity[18]. The ideal line profile is illustrated with the dashed line.

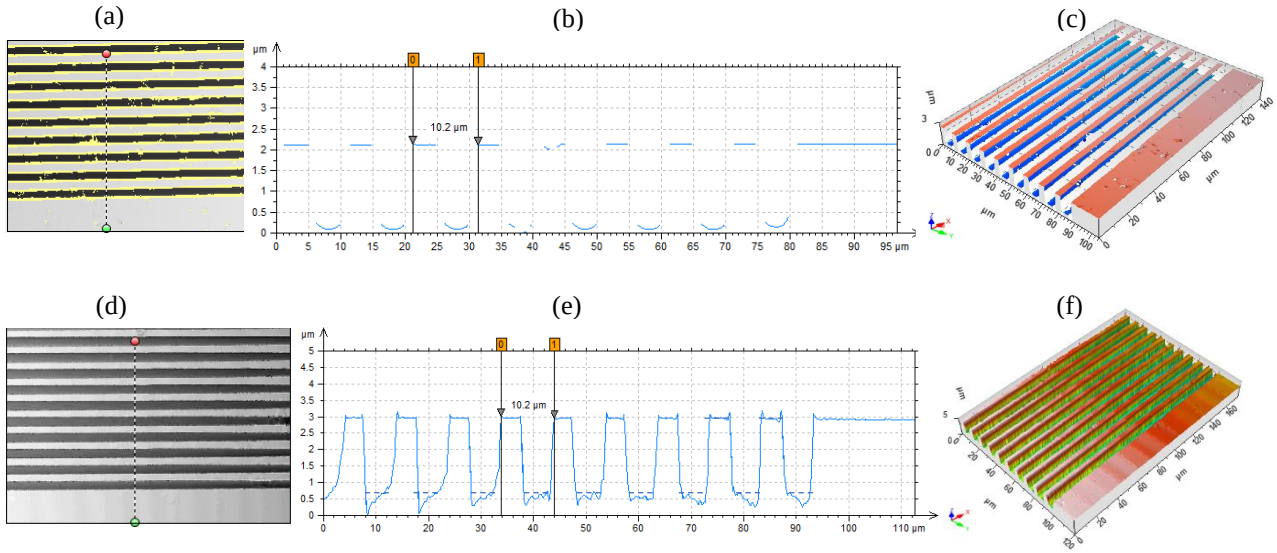

Figure *8*. Etched Silicon, 10 µm pitch of grating and 2.2 µm, is measured using (a), (b), (c) a commercial microscope Zygo NewView 7200 in air (×50 Mirau, NA=0.55) and (d), (e), (f) ×40 water immersion Linnik system (NA=0.8, λ_{eff}=450 nm).

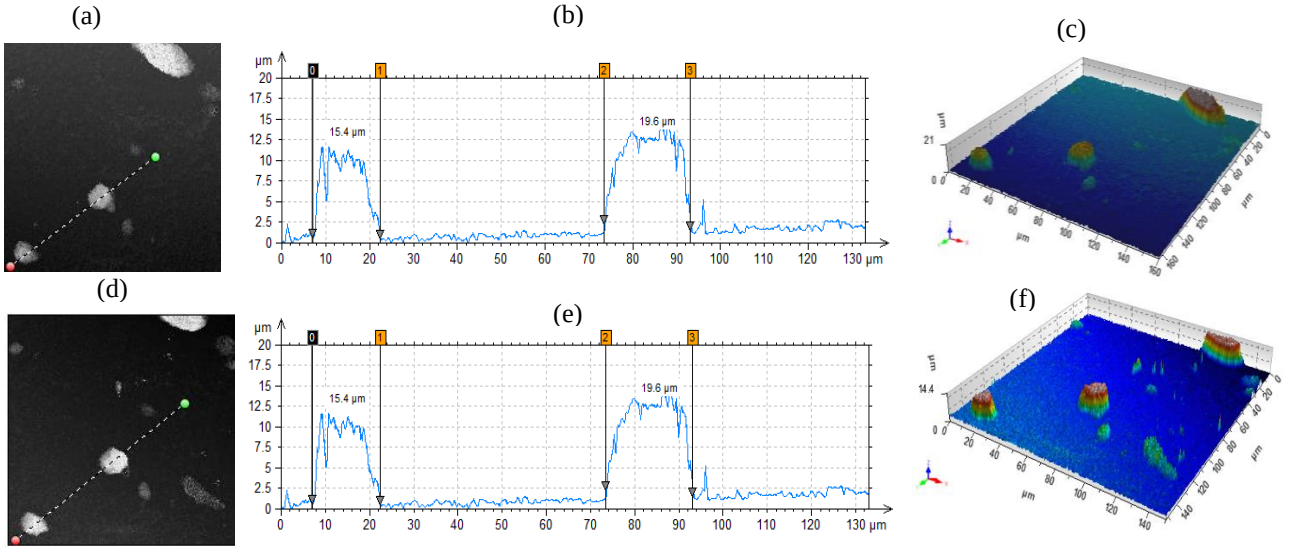

Figure *9*. An aggregate layer of 1 g/l alumina is measured using (a), (b), (c) a modified Leitz-Linnik microscope in air (×50, NA=0.85, λ_{eff}=720 nm); and (d), (e), (f) immersion Linnik system in water (×40, NA=0.8, λ_{eff}=450 nm).

However, using the immersion Linnik results in a better profile of the surface than the Zygo microscope. We can observe that the line profile in Figure *8* (e) is much better than in *Figure 8* (b) due to the improved lateral resolution.

Despite there being some artefacts in the profiling images, the comparisons of the line profiles between the new immersion Linnik system and the other microscopes show a similar range in the results on the same area of the sample surface. Whilst Figure 9 presents a better altitude image in water, a better contrast image of the colloid is obtained when measured in water. This result demonstrates the opportunity of studying colloids or other materials that can be measured in water or liquid.

4. CONCLUSIONS

In this paper, we have presented a new measurement system of a water immersion Linnik using elastic polymer path length compensation for 3D profiling of materials and colloidal samples in water. The use of self-supporting SPA and PDMS slabs between the reference mirror and the objective for compensating the optical path difference provide a convenient alternative solution to that of water without the problems of leakage. The first results of the system in measuring etched silicon holes and colloid layers show better image quality for the measurments in water. This opens the possibility of characterizing chemical and biological phenomena in liquid at high resolution using an optical non-contacting and non-invasive technique.

ACKNOWLEDGEMENTS

We would like to thank Catherine Galindo (IPHC) for help in the preparation of the colloidal layers of alumina and Florent Dietrich for help in making the PDMS mold. We also thank to Pierre Pfeiffer (ICube) for helping to do the measurements by AFM and Zygo microscopes.

REFERENCES

[1] Dubois, A., Grieve, K., Moneron, G., Lecaque, R., Vabre, L., and Boccara, C., "Ultrahigh-resolution full-field optical coherence tomography," *Appl. Opt.*, vol. 43, 2874–2883 (2004).
[2] Kittang, L.O.O., "Development and testing of a Linnik Interference Microscope for Sub-surface Inspection of Silicon during moving Indentation," (2012).
[3] Niehues, J., Lehmann, P., and Xie, W., "Low coherent Linnik interferometer optimized for use in Nano Measuring Machines," in *56th IWK, International Scientific Colloquium* (2013).
[4] Dubois, A., "Full-Field Optical Coherence Microscopy," in *Selected Topics in Optical Coherence Tomography, INTECH*, pp. 3–20 (2012).
[5] Sinclair, M.B., De Boer, M.P., and Corwin, A.D., "Long-working distance incoherent-light interference microscope," Appl. Opt., vol. 44, 7714–7721 (2005).
[6] Lazarev, G., and Sedashev, A., "Laser microinterferometer for estimation of red blood cell volume," in *Optical Technologies in Biophysics and Medicine VIII*, 653516-653516–7 (2007).
[7] Pezzaniti, J.L., and Chipman, R.A., "Angular dependence of polarizing beam-splitter cubes.," Appl. Opt., vol. 33, no. 10, 1916–1929 (1994).
[8] Motamedi, M.E., and Schwider, J., "Micro-Optic component, testing, and applications," in MOEMS: Micro-opto-electro-mechanical systems, M. E. Motamedi, Ed. Bellingham: SPIE Press (2005).
[9] de Groot, P.J. and Biegen, J.F., "Interference microscope objectives for wide-field areal surface topography measurements," *Opt. Eng.*, vol. 55, no. 7, 74110 (2016).
[10] Montgomery, P., Anstotz, F., Montagna, J., Montaner, D., Pramatarova, L., and Pecheva, E., "Towards real time 3D quantitative characterisation of in situ layer growth using white light interference microscopy," *J. Phys.*, vol. 253 (2010).
[11] Oh, W.Y., Bouma, B.E., Iftimia, N., Yun, S.H., Yelin, R., and Tearney, G.J., "Ultrahigh-resolution full-field optical coherence microscopy using InGaAs camera," Opt. Express, vol. 14, no. 2, 13–19, 2006.

[12] Byeong-il, L. *et al.*, "Feasibility of Full-field Optical Coherence Microscopy in Ultra-structural Imaging of Human Colon Tissues," *J. Korean Phys. Soc.*, vol. 57 (2010).
[13] Chen, Y., Huang, S.W., Zhou, C., Potsaid, B., and Fujimoto, J.G., "Improved Detection Sensitivity of Line-Scanning Optical Coherence Microscopy," *IEEE J Sel Top Quantum Electron*, vol. 18, no. 3, 1094–1099 (2012).
[14] Ogien, J., "Développement de systèmes de microscopir par cohérence optique pour l'imagerie de la peau," Université Paris-Saclay, 2017
[15] Ogien, J. and Dubois, A., "High-resolution full-field optical coherence microscopy using a broadband light-emitting diode," Opt. Express, vol. 24, no. 9, p. 9922 (2016).
[16] Medina-Torres, L., Calderas, F., Sanchez-Olivares, G., and Nuñez-Ramirez, D.M., "Rheology of sodium polyacrylate as an emulsifier employed in cosmetic emulsions," Ind. Eng. Chem. Res., vol. 53, no. 47, 18346–18351 (2014).
[17] Guellil, M., Montgomery, P.C., Pfeiffer, P., and Serio, B., "Comparison of areal measurements of the same zone of etched Si and hydroxyapatite layers on etched Si using different profiling techniques," in Optical micro and nanometrology V (2014).
[18] Petzing, J., Coupland, J.M., and Leach, R.K., The measurement of rough surface topography using coherance scanning interferometry, no. 116. National Physical Laboratory, 2010.